

Energy release rate for kinking crack using mixed finite element

Bouziane Salah^{*1}, Bouzerd Hamoudi¹, Boulares Noureddine¹
and Guenfoud Mohamed²

¹Department of Civil Engineering, University of 20 August 1955 Skikda, Skikda, Algeria

²Laboratory of Civil Engineering and Hydraulics, University of Guelma, Guelma, Algeria

(Received December 27, 2013, Revised March 9, 2014, Accepted March 20, 2014)

Abstract. A numerical method, using a special mixed finite element associated with the virtual crack extension technique, has been developed to evaluate the energy release rate for kinking cracks. The element is two dimensional 7-node mixed finite element with 5 displacement nodes and 2 stress nodes. The mixed finite element ensures the continuity of stress and displacement vectors on the coherent part and the free edge effect. This element has been formulated starting from a parent element in a natural plane with the aim to model different types of cracks with various orientations. Example problems with kinking cracks in a homogeneous material and bimaterial are presented to assess the computational accuracies.

Keywords: mixed finite element; kinking crack; energy release rate; virtual crack extension technique; bimaterial

1. Introduction

The problem of kinking cracks is relevant to situations where cracks change direction from the original orientation. The problem has received a considerable attention for analytical study. This problem has been solved by Chatterjee (1975), Amestoy and Leblond (1992) using the conformal mapping technique. Vitek (1977), Lo (1978), Hayashi and Nemat-Nasser (1981), Melin (1986) studied the problem with methods based on continuous distributions of dislocations. Cotterel and Rice (1980) solved the problem using perturbation techniques, Theocaris and Makrakis (1986, 1987) used the Mellin transform. Khrapkov (1971) proposed a solution based on Mellin transform and Bilby and Cardew (1975) used the Khrapkov's solution to solve the problem of semi-infinite kinked crack (Blanco *et al.* 1998). Li *et al.* (2010) presented a solution for the elastic T-stress at tip of a slightly curved or kinked based on a perturbation approach. Beghini *et al.* (2012) proposed a simplified approach for evaluating the stress intensity factors of an inclined edge kinked crack in a semi-plane. This method is based on an analytical weight function.

Numerical analysis of the crack kinking using finite element has not received much attention. Maiti (1990) used three different methods: stiffness derivative procedure, J integral method and crack closure integral technique to approximate energy release rate for a crack kinks away from its original direction. Xie *et al.* (2004) proposed a numerical method based on the virtual crack

*Corresponding author, Ph.D., E-mail: bouziane_21@yahoo.fr

closure technique and in conjunction with the finite element to compute strain energy release rates for cracks that kink. Jakobsen *et al.* (2008) studied a general interface delamination and crack kinking from an inclined core junction in a sandwich beam. A finite element model was developed and calibrated against a known model by He and Hutchinson (1989). Bäker (2008) used the energy release rate to determine the crack propagation direction. In two dimensions, this can be considered as one-dimensional optimization problem where the kinking angle is chosen to maximize the energy release. Bäker (2009) presented a method to calculate crack directions by using trial cracks. This approach is applied to three different situations: the kinking angle of a crack loaded under mixed mode load, the kinking angle of a crack near a bimaterial interface, and crack propagation at the interface of an elastic inclusion. Marsavina *et al.* (2009) used the finite element method to calculate the stress intensity factors at the tips of crack. The effects of material properties, the kinked crack length, the interface crack length, and the kinked angle were investigated. Boulenouar *et al.* (2013) proposed a numerical modeling of crack propagation under mixed mode loading conditions. This approach is based on the implementation of the displacement extrapolation method and the strain energy density theory in a finite element code. At each crack increment length the kinking angle is evaluated as a function of stress intensity factors.

This paper deals with the problem of kinking cracks. A special mixed finite element, based on Reissner's mixed variational principle, has been associated with the virtual crack extension method to evaluate the energy release rate for kinking cracks. This mixed finite element takes into account the continuity of the interface on the coherent part (mechanical and geometrical continuity) and the discontinuity of this one on the cracked part (free edge effect). This element was initially developed by Bouzerd (1992) using a direct formulation: the shape functions of the displacement and stress fields are built directly starting from the real configuration of the element in a physical (x, y) plane.

The present element was reformulated by Bouziane *et al.* (2009) starting from a parent element in a natural (ζ, η) plane. This formulation presents, in addition to the simplification of calculations, the enormous advantage of modelling different types of cracks with various orientations. The accuracy of the new numerical method has been evaluated by comparing the numerical solution with available analytical solutions or numerical ones obtained from others methods in example problems with kinking cracks in homogeneous materials and bimetals.

2. Mixed finite element

The mixed finite element RMQ-7 (Reissner Modified Quadrilateral) is a quadrilateral mixed finite element with 7 nodes and 14 degrees of freedom (Bouzerd 1992). The final configuration of the element, in a natural (ζ, η) plane, was obtained after passage by three following stages as showed in Fig. 1 (Bouziane *et al.* 2009):

1. Construction of a parent mixed finite element;
2. Relocalisation of some static variables from corners to the inside of the element;
3. Static condensation of the internal unknown variables.

Then, three of its sides are compatible with linear traditional displacement elements and present a cinematic node at each corner. The fourth side, in addition to its two displacement nodes of corner (node 1 and node 2), offers three additional nodes: a median node (node 5) and two intermediate nodes in the medium on each half-side (nodes 6 and 7), introducing the components of the stress vector along the interface. The formulation and the validation of the element have

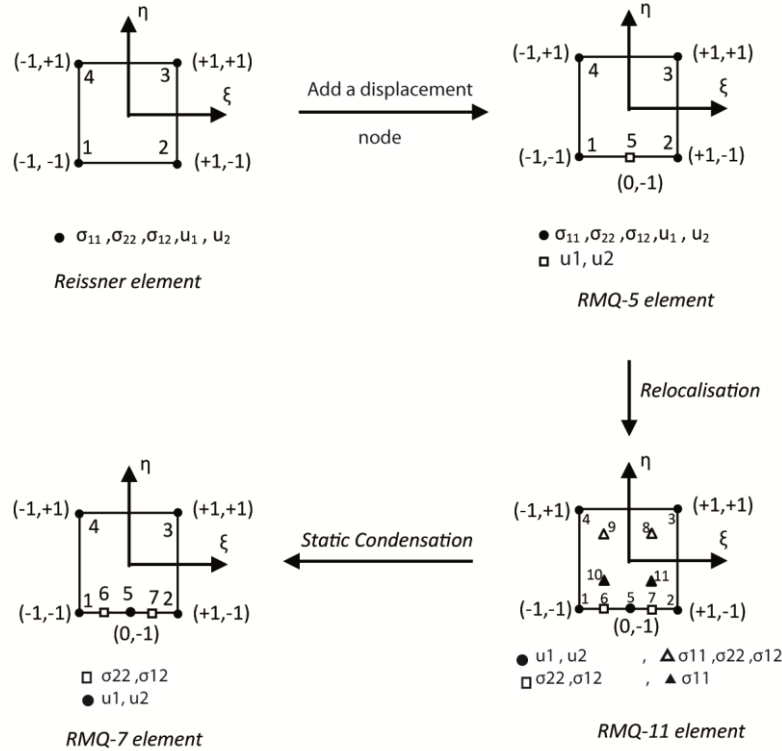


Fig. 1 Stages of construction of the mixed finite element

been presented by Bouziane *et al.* (2009).

The element displacement component is approximated by

$$\{u\} = [N]\{q\} \tag{1}$$

where $\{q\}^T = \{u_1^1, u_2^1, u_1^2, u_2^2, u_1^3, u_2^3, u_1^4, u_2^4, u_1^5, u_2^5\}$ is the vector of nodal displacements and $[N]$ is the matrix of interpolation functions for displacements.

The shape functions are

$$\begin{aligned}
 N_1 &= \frac{1}{2}(1 - \xi)(1 - \eta)\xi \quad , \quad N_2 = \frac{1}{4}(1 + \xi)(1 - \eta)\xi \quad , \quad N_3 = \frac{1}{4}(1 + \xi)(1 + \eta) \\
 N_4 &= \frac{1}{4}(1 - \xi)(1 + \eta) \quad , \quad N_5 = \frac{1}{2}(1 - \xi^2)(1 - \eta)
 \end{aligned}
 \tag{2}$$

The stress field in any point is written

$$\{\sigma\} = [M]\{\tau\} \tag{3}$$

where $[M]$ is the matrix of interpolation functions for stresses and $\{\tau\}$ vector of nodal stresses.

In the configuration of Fig. 1, the shape functions used to approximate σ_{11} are given by

$$\begin{aligned}
 M_{11}^8 &= \frac{1}{4}(1 + 2\xi)(1 + 2\eta) \quad , \quad M_{11}^9 = \frac{1}{4}(1 - 2\xi)(1 + 2\eta) \\
 M_{11}^{10} &= \frac{1}{4}(1 - 2\xi)(1 - 2\eta) \quad , \quad M_{11}^{11} = \frac{1}{4}(1 + 2\xi)(1 - 2\eta)
 \end{aligned}
 \tag{4}$$

The shape functions used to calculate σ_{12} and σ_{22} are given as follows

$$\begin{aligned} M_{i2}^6 &= \frac{1}{6}(1 - 2\xi)(1 - 2\eta) \quad , \quad M_{i2}^7 = \frac{1}{6}(1 + 2\xi)(1 - 2\eta) \\ M_{i2}^8 &= \frac{1}{3}(1 + 2\xi)(1 + \eta) \quad , \quad M_{i2}^9 = \frac{1}{4}(1 - 2\xi)(1 + \eta) \quad , \quad i = 1,2 \end{aligned} \quad (5)$$

The nodal approximation of the displacement and stress fields is expressed by

$$\begin{Bmatrix} \{\sigma\} \\ \{\varepsilon\} \end{Bmatrix} = \begin{bmatrix} [M] & [0] \\ [0] & [B] \end{bmatrix} \begin{Bmatrix} \{\tau\} \\ \{q\} \end{Bmatrix} \quad (6)$$

where $[B]$ is the strain-displacement transformation matrix.

The element matrix $[K_e]$ is given by

$$[K_e] = \begin{bmatrix} [K_{\sigma\sigma}] & [K_{\sigma u}] \\ [K_{\sigma u}]^T & [0] \end{bmatrix} \quad (7)$$

Here

$$[K_{\sigma\sigma}] = -t \int_{A_e} [M]^T [S] [M] dA^e \quad (8)$$

and

$$[K_{\sigma u}] = t \int_{A_e} [M]^T [B] dA^e \quad (9)$$

where: t is the thickness, $[S]$ is the compliance matrix, A^e is the element area and T indicate the matrix transpose.

3. Methodology of numerical calculation of G

3.1 Virtual crack extension method

The virtual crack extension method has been proposed by Parks (1974), Hellen (1975) to calculate the energy release rate (G).

At first, the deformation energy $\pi(a)$ is evaluated taking into account the crack initial configuration, where « a » is the length. Secondly the deformation energy $\pi(a + \delta a)$ is calculated in the modified state, where, the new configuration of the crack has a length of « $a + \delta a$ » where δa is an infinitesimal displacement of the crack tip. The energy released due to this length variation is equal to

$$\delta\pi = \pi(a) - \pi(a + \delta a) \quad (10)$$

The energy release rate G is obtained with the following relation:

$$G = \delta\pi / \delta a \quad (11)$$

3.2 Evaluation of energy release rate G

The virtual crack extension method associated with the RMQ-7 element is used to calculate the

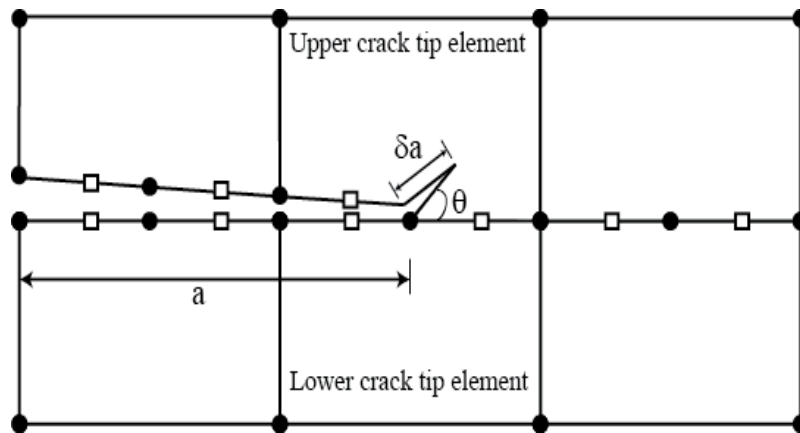
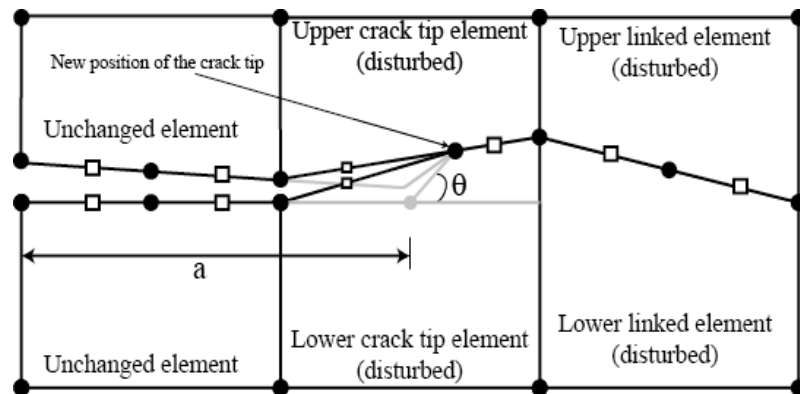
Fig. 2 Crack geometry for a kinking (extension δa)

Fig. 3 Reorganization of the mesh around the new tip crack

energy release rate G in the case of kinking.

In the case of a co-linear extension of the crack, Bouzard (1992) showed that a single discretisation is sufficient to evaluate the energy release rate. In the present work, the same procedure is adopted with some modifications added in order to take into account the non co-linear extension of the crack as showed in Fig. 2 (Bouzard *et al.* 2011).

By considering a crack extension δa , following a specified direction with an angle θ with the initial extension (Fig. 2). The new situation can be represented by an oblique segment beginning at node 1 of the upper crack tip element, and following the path of the new position of the crack tip after extension, as showed in Fig. 3.

This approximation is quite acceptable, as long as δa is small. That is why the choice of δa has an important role in our study. Theoretically, the value of δa must be taken as small as possible, in order to numerically represent the Eqs. (10)-(11).

This geometric approximation requires a meshing rearrangement around the tip crack involving only four (4) elements: the two elements (upper and lower) belonging to the crack tip and the two elements directly linked to them in the direction of the crack extension, the remaining meshing is unchanged, as showed in Fig. 3.

The energy release rate G is calculated by means of the method elaborated by Bouzard (1992).

It is evaluated by taking the parameters in the « $a + \delta a$ » configuration with kinking. In this study the « a » configuration is implicitly used by canceling δa and storing the elementary matrices of the concerned elements.

Indeed, with the assumptions of the linear elastic behaviour in small displacements, the solutions $v(a)$ and $v(a + \delta a)$ obtained in the structure with a crack length of " a " and in the same structure with a crack length " $a + \delta a$ " are quite similar especially when the variation δa is smaller in contrast with the dimensions of the crack tip.

We can write with a reasonable approximation that

$$v(a) = v(a + \delta a) \quad (12)$$

Different examples have been treated and the results confirmed the Eq. (12) which is theoretically coherent and physically acceptable; as long as the conditions used are respected. Petit (1990) used an identical process in the analysis of cracked structures.

If we consider that the external loading do not vary during the extension δa , then the energy release rate G is calculated as follows

$$G = - \frac{\pi(a+\delta a) - \pi(a)}{\delta a} \quad (13)$$

where $\pi(a + \delta a)$ and $\pi(a)$ represent respectively the deformation energy of the cracked structure in the study cases « $a + \delta a$ » and « a ». In its discretised form, the deformation energy is

$$\pi = \frac{1}{2} \sum_{i=1}^{ne} \{v\}_i^T [K]_i \{v\}_i \quad (14)$$

with:

ne = total number of elements in discretized structure,

$\{v\}_i$ = vertical vector containing the nodal values of element i ,

$[K]_i$ = elementary matrix of element i , and the exponent T indicates the transposed vector.

By substituting Eq. (14) in Eq. (13), the energy release rate G relation becomes

$$G = - \frac{1}{2\delta a} \left[\sum_{i=1}^{ne} \{v(a+\delta a)\}_i^T [K(a+\delta a)]_i \{v(a+\delta a)\}_i - \sum_{i=1}^{ne} \{v(a)\}_i^T [K(a)]_i \{v(a)\}_i \right] \quad (15)$$

Taking into account Eq. (12), the relation (15) can be written as follows

$$G = - \frac{1}{2\delta a} \sum_{i=1}^{ne} \{v(a+\delta a)\}_i^T \left[[K(a+\delta a)]_i - [K(a)]_i \right] \{v(a+\delta a)\}_i \quad (16)$$

Because, only the elements of crack tip and the elements immediately linked to them are disturbed (Fig. 3), then G can be recalculated by means of the following relation:

$$G = - \frac{1}{2\delta a} \sum_{f=1}^{nf} \{v(a+\delta a)\}_f^T \left[[K(a+\delta a)]_f - [K(a)]_f \right] \{v(a+\delta a)\}_f \quad (17)$$

where nf is the number of elements concerned by the disturbance δa , following the inclined extension of the crack. In Fig. 3, we notice that $nf = 4$.

Eq. (17) shows that only the elements concerned by the disturbance of the crack are used to compute the energy release rate. Following this, it is necessary to evaluate their elementary matrices in the configuration « a » and the energy release rate is calculated using Eq. (17); by means of a unique discretisation, after a difference calculation of the elementary matrices of the concerned elements only; representing the states « $a + \delta a$ » and « a ».

The relation (17) can be written as

$$G = -\frac{1}{2} \sum_{f=1}^{n_f} \{v\}_f^T \left[\frac{\delta K_f}{\delta a} \right] \{v\}_f \quad (18)$$

In practice, the discretisation of the cracked structure is done in the context « $a + \delta a$ ». Whereas, the configuration « a » is obtained in the same analysis by calculating and storing the elementary matrices of the concerned elements by taking $\delta a = 0$. Afterwards, at the resolution stage, the nodal values of the concerned elements are extracted and a special module will evaluate the energy release rate using the Eq. (18).

4. Validation of the method

The previously developed model is validated for a real case which consists on the study of the kinking of a central crack in a square plate for which an analytical solution has been established as well as a numerical analysis.

The study is about a square plate with a central crack which is subjected to normal tensile stress $\sigma = 10$ MPa, as shown in Fig. 4 (Xie *et al.* 2004). The geometric dimensions of the plate are:

- side length $2w = 200$ mm
- crack length $2a = 40$ mm

The plate is made of a homogeneous material or an isotropic bimaterial.

The analytical values of the energy release rate G has been calculated for different angles θ with the help of a subprogram on the basis of an exact solution taken in account by Xie *et al.* (2004). The out of plane extensions at 10° , 20° , 30° , 40° , 50° , 60° , 70° , 80° and 90° to the main crack have been examined.

The geometrical and mechanical symmetry permits to discretise only the half of the structure using mixed finite element presented above. After a convergence study, the mesh constituted by 4900 elements and 12441 nodes, has been retained.

4.1 Homogeneous material

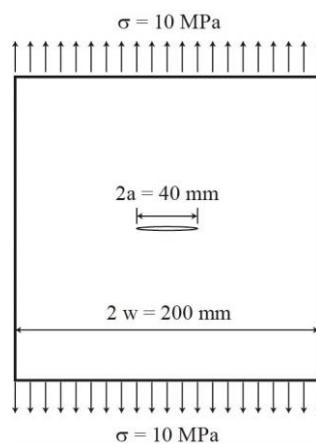


Fig. 4 Studied plate

Table 1 Energy release rate G for different values of kinking angles (case (a))

$\theta(^{\circ})$	G (N/mm) Proposed method	G (N/mm) Analytical solution	% differences with analytical solution
0	6.486	6.498	-0.185
10	6.390	6.400	-0.156
20	6.132	6.112	+0.327
30	5.630	5.657	-0.477
40	5.099	5.067	+0.631
50	4.407	4.384	+0.525
60	3.660	3.655	+0.137
70	2.920	2.926	-0.205
80	2.259	2.238	+0.938
90	1.626	1.625	+0.062

Table 2 Energy release rate G for different values of kinking angles (case (b))

$\theta(^{\circ})$	G (N/mm) Proposed method	G (N/mm) Analytical solution	% differences with analytical solution
0	1.622	1.625	-0.185
10	1.606	1.600	+0.375
20	1.533	1.528	+0.327
30	1.407	1.414	-0.495
40	1.275	1.267	+0.631
50	1.102	1.096	+0.547
60	0.915	0.914	+0.109
70	0.730	0.732	-0.273
80	0.565	0.560	+0.893
90	0.410	0.406	+0.985

The plate is made of a homogeneous and isotropic material. Two different cases were studied:

- Case (a): $E=1000$ MPa, $\nu=0,25$
- Case (b): $E=4000$ MPa, $\nu=0,25$

The numerical results obtained using the proposed method are compared with the analytical solution (Xie *et al.* 2004). Computed results are given in Tables 1 (case (a)) and 2 (case (b)).

The given results by the proposed approach are very close to those of analytical solution. These results obtained for various kinking angles (from 0° to 90°) with the ratio $\delta a/a$ varying from 1/50 to 1/700. Theoretically, more this ratio is small, more is the exactness of the model is established, but if it is too small, numerical disturbances can occur and distort the results.

The results shown in Tables 1 and 2 indicate that the gap with the exact solution remains confined between the values (in absolute value) 0.062% and 0.985%, what affirms that the results obtained are in excellent agreement with the exact solution.

Figs. 5-6 show the variation of the energy release rate G with the extension direction for a crack in the case (a) and case (b) respectively.

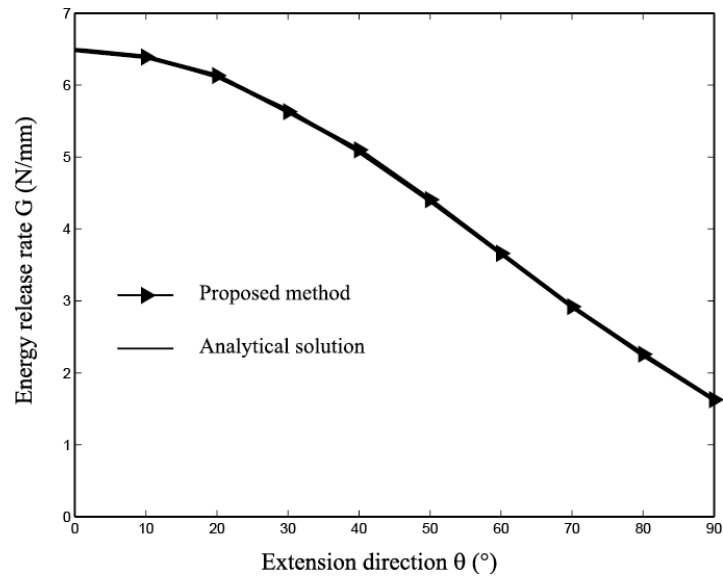


Fig. 5 Variation of energy release rate with different kinking angles (case (a))

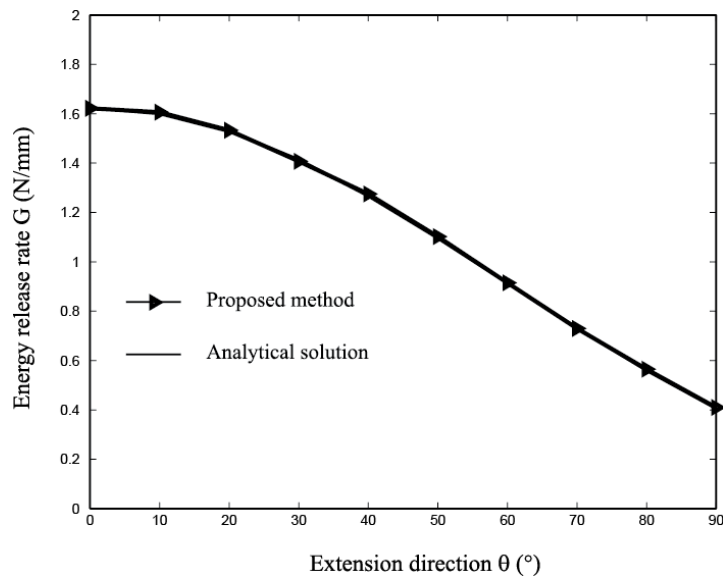


Fig. 6 Variation of energy release rate with different kinking angles (case (b))

It is seen that the present model computations are in very good agreement with the analytical solution.

For the case $\theta=0^{\circ}$, the exact solution (Xie *et al.* 2004) of the energy release rate G is compared with the results obtained using J -integral method computed from ABAQUS (Xie *et al.* 2004) where the discretisation required 27000 nodes, the one and two-step approach based on the crack virtual closure technique (Xie *et al.* 2004) and the values obtained by the present method.

Table 3 Values of the energy release rate G for $\theta=0^\circ$ (case (a))

$\theta=0^\circ$	Energy release rate $G(\text{N/mm})$	% difference with analytical solution
One -step-analysis (Xie <i>et al.</i> 2004)	6.515	+ 0.262
Two -step-analysis (Xie <i>et al.</i> 2004)	6.612	+ 1.754
J -integral from ABAQUS (Xie <i>et al.</i> 2004)	6.507	+ 0.139
Proposed method	6.486	- 0.185
Analytical solution	6.498	/

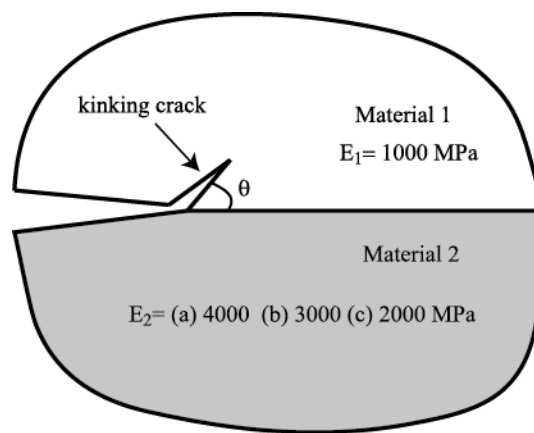


Fig. 7 Bimaterial with kinking crack

Calculated results for the case (a) are given in Table 3.

The obtained values ($\theta = 0^\circ$) for the present model are in very good agreement with the exact solution compared to those obtained by one and two-step approach (Xie *et al.* 2004) and the J -integral method from ABAQUS (Xie *et al.* 2004), even with a number of nodes, i.e., a number of degrees of freedom, largely inferior (12441 compared to 27000 for ABAQUS (Xie *et al.* 2004)) and with a single discretisation using the proposed mixed finite element. It is seen that the present approach is an accurate procedure for computing the energy release rate.

4.2 Isotropic bimaterial

The plate is made of an isotropic bimaterial as shown in Fig. 7. Three different cases were studied:

- Case (a): $E_1=1000 \text{ MPa}$, $\nu_1=0.25$, $E_2=4000 \text{ MPa}$, $\nu_2=0.25$, $E_2/E_1=4$
- Case (b): $E_1=1000 \text{ MPa}$, $\nu_1=0.25$, $E_2=3000 \text{ MPa}$, $\nu_2=0.25$, $E_2/E_1=3$
- Case (c): $E_1=1000 \text{ MPa}$, $\nu_1=0.25$, $E_2=2000 \text{ MPa}$, $\nu_2=0.25$, $E_2/E_1=2$

The numerical results of the energy release rate G using the proposed method are compared with the analytical solutions for the crack along the interface ($\theta = 0^\circ$), and the results evaluated with the J -integral method computed from ABAQUS (Xie *et al.* 2004) and those calculated using the one and two-step approach based on the crack virtual closure technique (Xie *et al.* 2004). Computed results for case (a) are given in Table 4. The G values provided by the proposed method

Table 4 Values of the energy release rate G for $\theta=0^\circ$ (case (a))

$\theta=0^\circ$	Energy release rate G (N/mm)	% difference with analytical solution
One -step-analysis (Xie <i>et al.</i> 2004)	3.823	-2.92
Two -step-analysis (Xie <i>et al.</i> 2004)	3.886	-1.32
J-integral from ABAQUS (Xie <i>et al.</i> 2004)	3.829	-2.77
Proposed method	3.953	+0.381
Analytical solution	3.938	/

Table 5 Values of the energy release rate G for different case ($\theta=0^\circ$)

$\theta=0^\circ$	G (N/mm) Proposed method	G (N/mm) Analytical solution	% differences with analytical solution
Case (a)	3.953	3.938	+0.381
Case (b)	4.260	4.241	+0.448
Case (c)	4.838	4.828	+0.207

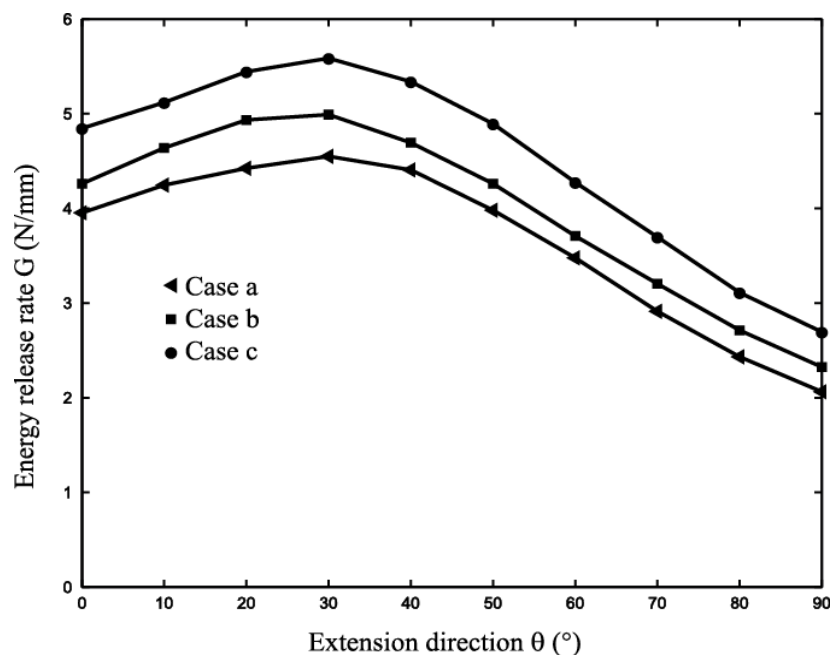


Fig. 8 Variation of energy release rate with extension direction for different case

for bimetals confirm the excellent results of the homogeneous case.

Table 5 gives the values of the energy release rate G for different case. The numerical results are compared with the analytical solution for the crack along the interface.

The accuracy of computational results is very good compared with the analytical solution. The errors with respect to the exact solution ranges from +0.207% to +0.448% for the different case.

Fig. 8 show the variation of the energy release rate G with the extension direction for a crack in the different case.

The figures obtained show a shape different from that of the homogeneous case. They increase to lead to a peak then decrease. In the homogeneous case the curves continuously decrease from the maximum value obtained for $\theta = 0^\circ$, what means that if there is propagation it will be done in initial direction of the crack.

As for the case (a) studied by Xie *et al.* (2004) in bimetals case, and according to the criterion of G_{max} , the kinking occurs according to an angle around 30° .

In all bimaterial cases the kinking grows into the material 1 who presents the weak mechanical characteristics.

The results obtained in this example of validation show that the proposed method is an accurate and an efficient procedure for computing the energy release rate for crack kinking problems.

5. Conclusions

A new numerical method, based on the virtual crack extension technique associated with a special mixed finite element, has been proposed to evaluate the energy release rate for kinking cracks. The present element is 7-node two dimensional mixed finite element with 5 displacement nodes and 2 stress nodes. In the formulation of this element, we used Reissner's mixed variational principle to build the parent element. The mixed interface finite element is obtained by successively exploiting the technique of localisation and the static condensation procedure.

This new technique makes it possible to evaluate energy release rate by only one finite elements analysis. Computed results show that the proposed method is an accurate and an efficient procedure for computing the energy release rate for crack kinking problems.

This approach is to be completed by an extension to the orthotropic and anisotropic bimetals case. It would be very interesting to study the influence of the ratio $\delta a/a$ and find an objective criterion for its choice.

A detailed study around the angle giving G_{max} must be conducted to evaluate the influence of strong material on the kinking angle.

References

- Amestoy, M. and Leblond, J.B. (1992), "Crack paths in plane situations-II. Detailed form of expansion of the stress intensity factors", *Int. J. Solid. Struct.*, **29**, 465-501.
- Bâker, M. (2008), "Finite element crack propagation calculation using trial cracks", *Comput. Mater. Sci.*, **43**, 179-183.
- Bâker, M. (2009), "Simulation of crack propagation in mixed mode and at biomaterial interfaces using trial cracks", *Comput. Mater. Sci.*, **45**, 680-683.
- Beghini, M., Benedetti, M., Fontanari, V. and Monelli, B.D. (2012), "Stress intensity factors of inclined edge cracks: A simplified approach", *Eng. Fract. Mech.*, **81**, 120-129.
- Bildy, B.A. (1975), "The crack with a kinked tip", *Int. J. Fract. Mech.*, **11**, 708-712.
- Blonco, C., Martinez-Esnaola, J.M. and Atkinson, C. (1998), "Kinked cracks in an anisotropic elastic materials", *Int. J. Fract.*, **93**, 387-407.
- Boulouar, A., Benseddiq, N. and Mazari, M. (2013), "Strain energy density prediction of crack propagation for 2D linear elastic materials", *Theor. Appl. Fract. Mech.*, **67-68**, 29-37.
- Bouzerd, H. (1992), "Elément fini mixte pour interface cohérente ou fissurée", Thèse de doctorat en Génie Civil, Université Claude Bernard Lyon I, France.

- Bouzerd, H., Boulares, N. and Bouchair, A. (2011), "Un élément fini mixte pour le calcul du taux de restitution d'énergie du cou dage (kinking) d'une fissure", *XXIXe Rencontres Universitaires de Génie Civil*, Tlemcen, Algérie.
- Bouziane, S., Bouzerd, H. and Guenfoud, M. (2009), "Mixed finite element for modelling interfaces", *Euro. J. Comput. Mech.*, **18**(2), 155-175.
- Chatterjee, S.N. (1975), "The stress field in the neighbour hood of a branched crack in a infinite elastic sheet", *Int. J. Solid. Struct.*, **11**, 512-538.
- Cotterel, B. and Rice, J.R. (1980), "Slightly curved or kinking cracks", *Int. J. Fract.*, **16**, 155-159.
- Hayashi, K. and Nemat-Nasser, S. (1981), "Energy release rate and crack kinking under combined loading", *J. Appl. Mech.*, **13**, 520-524.
- He, M. and Hutchinson, J.W. (1989), "Kinking of crack out of an interface", *J. Appl. Trans. ASME*, **56**(2), 270-278.
- Hellen, T.K. (1975), "On the method of virtual crack extensions", *Int. J. Numer. Meth. Eng.*, **9**(1), 187-208.
- Jakobsen, J., Andreasen, J.H. and Bozhevolnaya, E. (2008), "Crack kinking of delamination at an inclined core junction interface in sandwich beam", *Eng. Fract. Mech.*, **75**, 4759-4773.
- Khrapkov, A.A. (1971), "The first problem for a notch at the apex of an infinite wedge", *Int. J. Fract. Mech.*, **7**, 373-382.
- Li, D.F., Li, C.F., Qing, H. and Lu, J. (2010), "The elastic T-stress for slightly curved or kinked cracks", *Int. J. Solid. Struct.*, **47**, 1753-1763.
- Lo, K.K. (1978), "Analysis of branched cracks", *J. Appl. Mech.*, **45**, 797-802.
- Maiti, S.K. (1990), "Finite element computation of strain energy release rate for kinking of a crack", *Int. J. Fract.*, **43**, 161-174.
- Marsavina, L. and Sadowski, T. (2009), "Kinked crack at a bimaterial ceramic interface-numerical determination of fracture parameters", *Comput. Mater. Sci.*, **44**, 941-950.
- Melin, S. (1986), "On singular integral equations for kinked cracks", *Int. J. Fract.*, **30**, 57-65.
- Parks, D.M. (1974), "A stiffness derivative finite element technique for determination of elastic crack tip stress intensity factors", *Int. J. Fract.*, **10**(4), 487-502.
- Petit, C. (1990), "Modélisation des milieux composites multicouches fissurés par la mécanique de la rupture", Thèse de doctorat d'université, Université Blaise Pascal, France.
- Theocaris, P.S. and Makrakis, G.N. (1986), "The kinked crack solved by Mellin transform", *J. Elasticity*, **16**, 393-411.
- Theocaris, P.S. and Makrakis, G.N. (1987), "Crack kinking in anti-plane shear solved by Mellin transform", *Int. J. Fract.*, **34**, 251-262.
- Vitek, V. (1977), "Plane strain intensity factors for branched cracks", *Int. J. Fract.*, **13**, 481-501.
- Xie, D., Waas, A.M., Shahwan, K.W., Schroedre, J.A. and Boeman, R.G. (2004), "Computation of energy release rates for kinking cracks based on virtual crack closure technique", *CMES*, **6**(6), 515-524.